Aggregation-induced Emission-active Hyperbranched Poly(tetrahydro-pyrimidine)s Synthesized from Multicomponent Tandem Polymerization

Yuzhang Huang[a], Ping Chen[a], Bo Wei[a], Rongrong Hu[a*], and Ben Zhong Tang[a,b*]

[a] *State Key Laboratory of Luminescent Materials and Devices, Center for Aggregation-Induced Emission, South China University of Technology, Guangzhou 510641, China*
[b] *Department of Chemistry, Hong Kong Branch of Chinese National Engineering Research Center for Tissue Restoration and Reconstruction, The Hong Kong University of Science & Technology, Clear Water Bay, Kowloon, Hong Kong, China*

Ⓔ Electronic Supplementary Information

Abstract Hyperbranched polymer with highly branched three-dimensional topological structure, a large number of end groups, and multifaceted functionalities have gained much attention, while polymers with aggregation-induced emission (AIE) properties become a group of popular luminescent materials recently. The design and synthesis of AIE-active hyperbranched polymers, which combine the advantages of these two types of materials, are attractive but challenging. In this work, four hyperbranched poly(tetrahydropyrimidine)s were synthesized from the metal-free room temperature multicomponent tandem polymerization of diester group-activated internal alkyne, polyfunctional aromatic amines, and formaldehyde in methanol under the catalysis of acetic acid. Through different monomer combination and controlling the monomer loading order, hyperbranched polymers with various topological structures as well as sequences of different functional groups in the polymer backbone were obtained with high molecular weights (up to 3.0×10^4 g/mol) in high yields (up to 98%). The hyperbranched poly(tetrahydropyrimidine) emitted faintly in solution, while its luminescence was notably enhanced in the aggregated state, suggesting its typical aggregation-induced emission property. It is anticipated that the multicomponent polymerization may provide a synthetic platform for the construction of hyperbranched polyheterocycles with diverse structures and functionalities.

Keywords Hyperbranched polymer; Multicomponent tandem polymerization; Aggregation-induced emission; Polyheterocycle

INTRODUCTION

Hyperbranched polymers with many branching sites are a special kind of three-dimensional macromolecules. Compared with linear polymers, hyperbranched polymers enjoy low viscosity, good solubility, good dispersion, high flow denaturation, large number of terminal functional groups, and facile modification of the numerous end groups.[1] They can find wide applications in various fields including self-assembly, biomedicine, stimuli-responsive materials, and chemosensors.[2−12] The general strategy of constructing hyperbranched polymers is to adopt AB_n ($n \geq 2$) or $A_2 + B_n$ ($n \geq 3$) type monomers in an efficient polymerization to afford hyperbranched polymers with desired structures.[13] Extensive works about hyperbranched polyethers, polyglycerols, polythioethers, and conjugated hyperbranched poly(tetraphenylethene) have been reported, which generally involve efficient synthetic methods such as epoxide polymerization, click chemistry strategies, and the activated monomer strategies.[14−19]

Polymers with aggregation-induced emission (AIE) behavior have raised great interest recently and found various applications such as fluorescent sensors,[20−22] optoelectronic devices,[23−25] and bioimaging.[26−28] Unlike the traditional luminescent polymers with concentration-caused fluorescence quenching effect, AIE polymers show no emission in solution, but obvious luminescence in its aggregated form in poor solvent or solid states.[29] Although AIE polymers exhibit large potential as functional luminescent materials, AIE-active hyperbranched polymers are rarely reported due to the shortage of synthetic approaches. For example, A_2- and A_4-type tetraphenylethene-containing diyne or tetrayne monomers were used respectively to construct conjugated hyperbranched polymers with aggregation-enhanced emission properties through polycyclotrimerization of alkynes.[30,31] In these AIE-active hyperbranched polymers, tetraphenylethene moieties are connected through 1,2,4- or 1,3,5-substituted benzene ring as branching site, which exhibit enhanced fluorescence in the solid state and can be em-

* Corresponding authors: E-mail msrrhu@scut.edu.cn (R.H.)
E-mail tangbenz@ust.hk (B.Z.T.)

ployed for explosive detection and fluorescent photopattern.

Multicomponent polymerization (MCP), which utilizes three or more monomers to directly afford polymer product with complex structures, is a versatile synthetic approach and an ideal tool for the construction of hyperbranched polymers. MCP enjoys a series of advantages such as great structural diversity, various monomer combination strategies, high efficiency and convenience, mild condition, and environmental benefit.[32−35] Among the reported MCPs, multicomponent tandem polymerization (MCTP) which combines multiple-step reactions in a one-pot synthetic procedure,[36−38] possesses great potential in the synthesis of functional polymer materials. MCTP can apply to various reactions and monomers, greatly extending the product structure scope to conjugated polymers and sequence-controlled polymers.[39,40] Recently, we developed an efficient metal-free room temperature MCTP of ester group-activated internal alkyne, aromatic amine, and formaldehyde.[41] By changing the feeding order of different aromatic diamines, the amount of formaldehyde, and reaction temperature, a series of structure- and sequence-controlled polyheterocycles with unique luminescence behavior were obtained (Scheme 1).

In this work, attracted by the unique advantages and strong designability of MCTP, four hyperbranched polymers containing *in situ* constructed tetrahydropyrimidine rings were synthesized *via* the metal-free room temperature tandem polymerization of diester group-activated internal alkyne, formaldehyde, and A₂-, A₃-, or A₄- type aromatic amine monomers. By controlling the different combination of multifunctional monomers and monomer loading order, hyperbranched polyheterocycles with various topological structures and sequences of functional units were accessed. The hyperbranched polymer also possessed typical aggregation-induced emission property, which was faintly emissive in solution but showed enhanced emission in the aggregated state.

EXPERIMENTAL

Materials

4,4′-Methylenedianiline (TCI), acetylenedicarboxylic acid (Energy), tris(4-aminophenyl)amine (Energy), diethylene glycol monomethyl ether (Energy), formaldehyde (Alfa Aesar, 37% in aq. soln.), tetrakis(4-aminophenyl)methane (Accela ChemBio), *p*-toluenesulfonic acid (Energy), cyclohexane (Aladdin), *n*-hexane (Aladdin), acetic acid, and methanol were used as received without further purification.

Tetrahydrofuran (Aladdin) was treated with sodium benzophenone ketyl and distilled under nitrogen prior to use.

Characterization

FTIR spectra were measured on a Bruker Vector 33 FT-IR spectrometer. All ^{1}H- and ^{13}C-NMR spectra were measured on Bruker Avance 500 MHz NMR spectrometer using CDCl₃ as solvent and tetramethylsilane (TMS, $\delta = 0$) as internal reference. UV-Vis absorption spectra were recorded on a Shimadzu UV-2600 spectrophotometer. Fluorescence spectra were recorded on a Horiba Fluoromax-4 fluorescence spectrophotometer. Fluorescence quantum yields were measured using a Hamamatsu absolute photoluminescence quantum yield spectrometer C11347 Quantaurus-QY. The weight-average (M_w) molecular weights and polydispersity indices (PDI = M_w/M_n) of polymers were estimated by a Waters advanced polymer chromatography (APC) system. THF was used as eluent at a flow rate of 0.5 mL/min. The molecular weight was calibrated by a set of monodispersed linear polystyrenes standard samples covering the M_w range of 10^3-10^7 g/mol.

Synthetic Procedure of Bis[2-(2-methoxyethyoxy)-ethyl]but-2-ynedioate (1)

Bis[2-(2-methoxyethyoxy)ethyl]but-2-ynedioate **1** was synthesized according to the literature.[41] Acetylenedicarboxylic acid (2.28 g, 20.0 mmol), diethylene glycol monomethyl ether (6.95 mL, 60.0 mmol), *p*-toluenesulfonic acid (0.34 g, 2.0 mmol), and cyclohexane (50 mL) were added into a two-necked round-bottom flask. The mixture was stirred at 80 °C in air for 24 h, which was then cooled down to room temperature and extracted with water (50 mL) and ethyl acetate (50 mL × 3). The organic layers were combined and dried with MgSO₄. The solvent was removed under vacuum and the crude product was purified through silica-gel column chromatography (ethyl acetate:petroleum ether = 1:4, *V:V*). Compound **1** was obtained as a yellow liquid in 62% yield.

General Synthetic Procedure and Characterization Data of Hyperbranched Polymers (*hb*-P1−4)

The general procedure for the synthesis of hyperbranched poly(tetrahydropyrimidine)s is given below using the preparation of *hb*-P**1** as an example (Scheme 2). 4,4′-Methylenedianiline (**2**, 0.059 g, 0.3 mmol), and bis[2-(2-methoxyethyoxy)ethyl]but-2-ynedioate (**1**, 0.191 g, 0.6 mmol) were dissolved in 1 mL of methanol, which were stirred for 30 min at room temperature in air. Aqueous solution of formal-
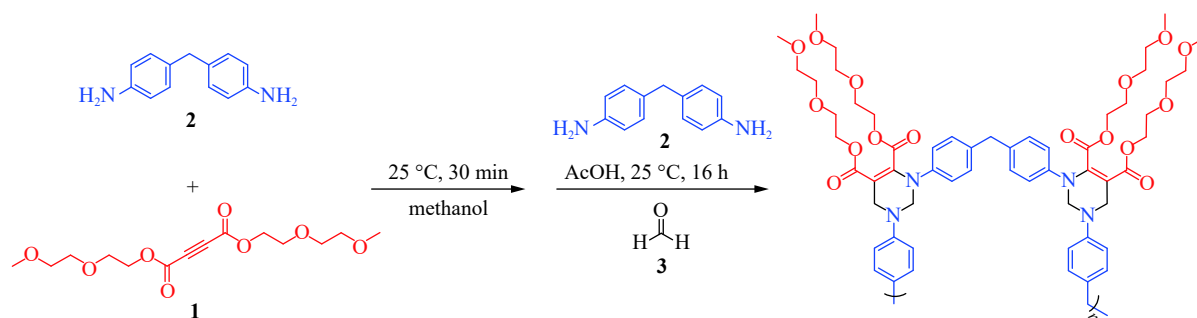
Scheme 1   The synthesis of sequence-controlled linear polymer through multicomponent tandem polymerization of activated alkyne, aromatic diamine, and formaldehyde
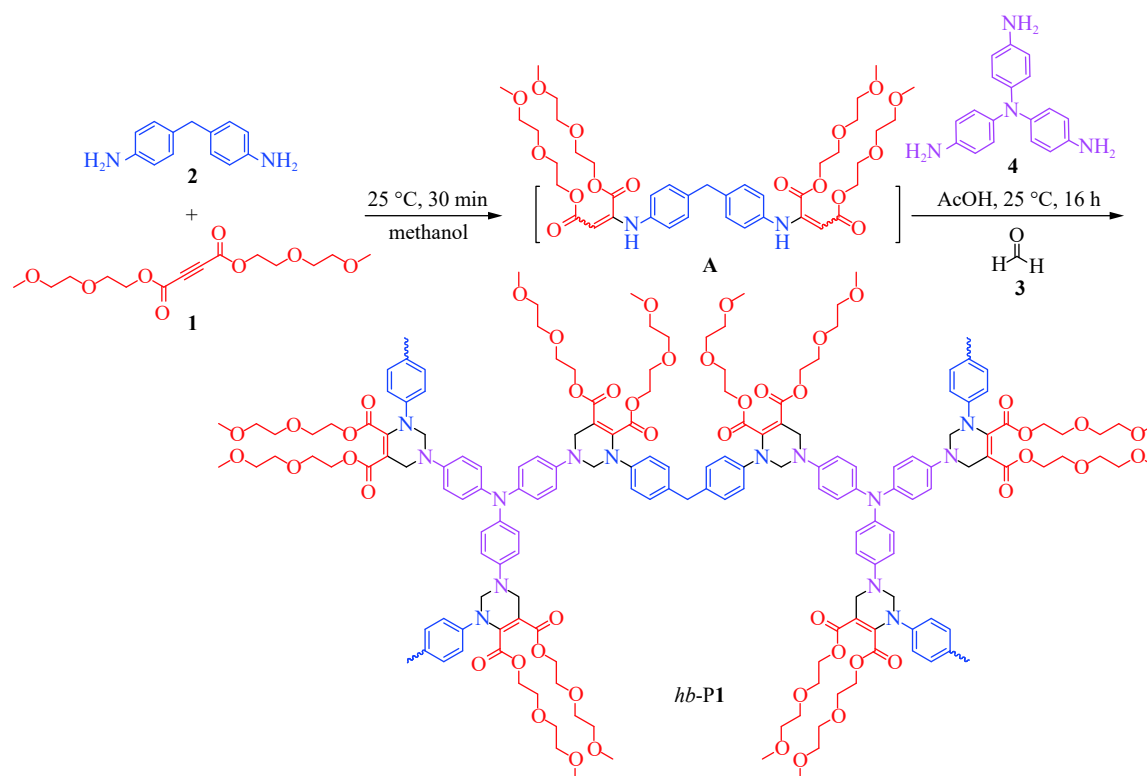
Scheme 2 The synthesis of hyperbranched polymer *hb*-P**1** through a one-pot MCTP

dehyde (**3**, 37 wt%, 136 μL, 1.8 mmol) and tris(4-amino-phenyl)amine (**4**, 0.058 g, 0.2 mmol) in 1 mL of methanol, and acetic acid (206 μL, 3.6 mmol) were then added into the mixture and the reaction solution was stirred for 16 h at room temperature in air. The mixture was diluted with 4 mL of dichloromethane and was then added into 100 mL of *n*-hexane through a cotton filter to precipitate the polymer product. The precipitates were allowed to stand for 3 h, followed by filtering and washing with 10 mL of *n*-hexane. The product was dried under vacuum at 25 °C for 12 h to afford *hb*-P**1**.

Characterization Data of *hb*-P1−4

Characterization data for hb-P1
A brown solid was obtained in 98% yield. M_w = 1.72 × 10^4 g/mol, M_w/M_n = 1.75. ^{1}H-NMR (CDCl$_3$, 500 MHz, TMS, δ, ppm): 7.12–6.90 (Ar−H), 6.90–6.70 (Ar−H), 6.58 (Ar−H), 4.80, 4.26 (CH$_2$), 4.16 (COO−CH$_2$), 4.12 (COO−CH$_2$), 3.86 (Ar−CH$_2$−Ar), 3.68 (CH$_2$), 3.61 (CH$_2$), 3.51 (CH$_2$), 3.44 (CH$_2$), 3.34 (CH$_3$), 3.31 (CH$_3$). ^{13}C-NMR (CDCl$_3$, 125 MHz, TMS, δ, ppm): 165.44 (C=O), 163.99 (C=O), 145.85, 143.30, 143.05, 142.89, 141.95, 141.53, 138.75, 129.75, 125.20, 124.63, 118.74, 117.72, 103.36, 71.82, 70.43, 70.27, 69.23, 68.36, 64.63, 63.32, 59.02 (CH$_3$), 48.12 (CH$_2$), 40.74 (Ar−CH$_2$−Ar). IR (KBr, *v*, cm^{-1}): 2881, 1741 (C=O), 1691 (C=O), 1587, 1506, 1450, 1394, 1261, 1211, 1107, 1033, 947, 823, 758, 719.

Characterization data for hb-P2
A brown solid was obtained in 84% yield. M_w = 1.17 × 10^4 g/mol, M_w/M_n = 1.60. ^{1}H-NMR (CDCl$_3$, 500 MHz, TMS, δ, ppm): 7.16–6.61 (Ar−H), 4.79, 4.22 (CH$_2$), 4.15 (COO−CH$_2$), 3.81 (Ar−CH$_2$−Ar), 3.70 (CH$_2$), 3.63 (CH$_2$),

3.53 (CH$_2$), 3.44 (CH$_2$), 3.37 (CH$_2$), 3.29 (CH$_3$), 3.26 (CH$_3$). IR (KBr, *v*, cm^{-1}): 3124, 2877, 1737 (C=O), 1685 (C=O), 1581, 1506, 1456, 1389, 1259, 1205, 1105, 1028, 935, 727.

Characterization data for hb-P3
A yellow solid was obtained in 94% yield. M_w = 2.24 × 10^4 g/mol, M_w/M_n = 2.08. ^{1}H-NMR (CDCl$_3$, 500 MHz, TMS, δ, ppm): 7.15–6.67 (Ar−H), 6.56 (Ar−H), 4.97–4.64, 4.27 (CH$_2$), 4.19 (COO−CH$_2$), 4.13 (CH$_2$), 3.84 (Ar−CH$_2$−Ar), 3.63 (CH$_2$), 3.53 (CH$_2$), 3.48 (CH$_3$), 3.32 (CH$_3$). IR (KBr, *v*, cm^{-1}): 3130, 2920, 1741 (C=O), 1687 (C=O), 1573, 1508, 1402, 1269, 1198, 1064, 923, 812.

Characterization data for hb-P4
A brown solid was obtained in 95% yield. M_w = 3.00 × 10^4 g/mol, M_w/M_n = 3.85. ^{1}H-NMR (CDCl$_3$, 500 MHz, TMS, δ, ppm): 7.19–6.46 (Ar−H), 4.78, 4.27 (CH$_2$), 4.17 (COO−CH$_2$), 3.69 (CH$_2$), 3.63 (CH$_2$), 3.53 (CH$_2$), 3.45 (CH$_2$), 3.36 (CH$_2$), 3.28 (CH$_3$). IR (KBr, *v*, cm^{-1}): 2893, 1739 (C=O), 1693 (C=O), 1579, 1502, 1259, 1207, 1080, 827, 723.

RESULTS AND DISCUSSION

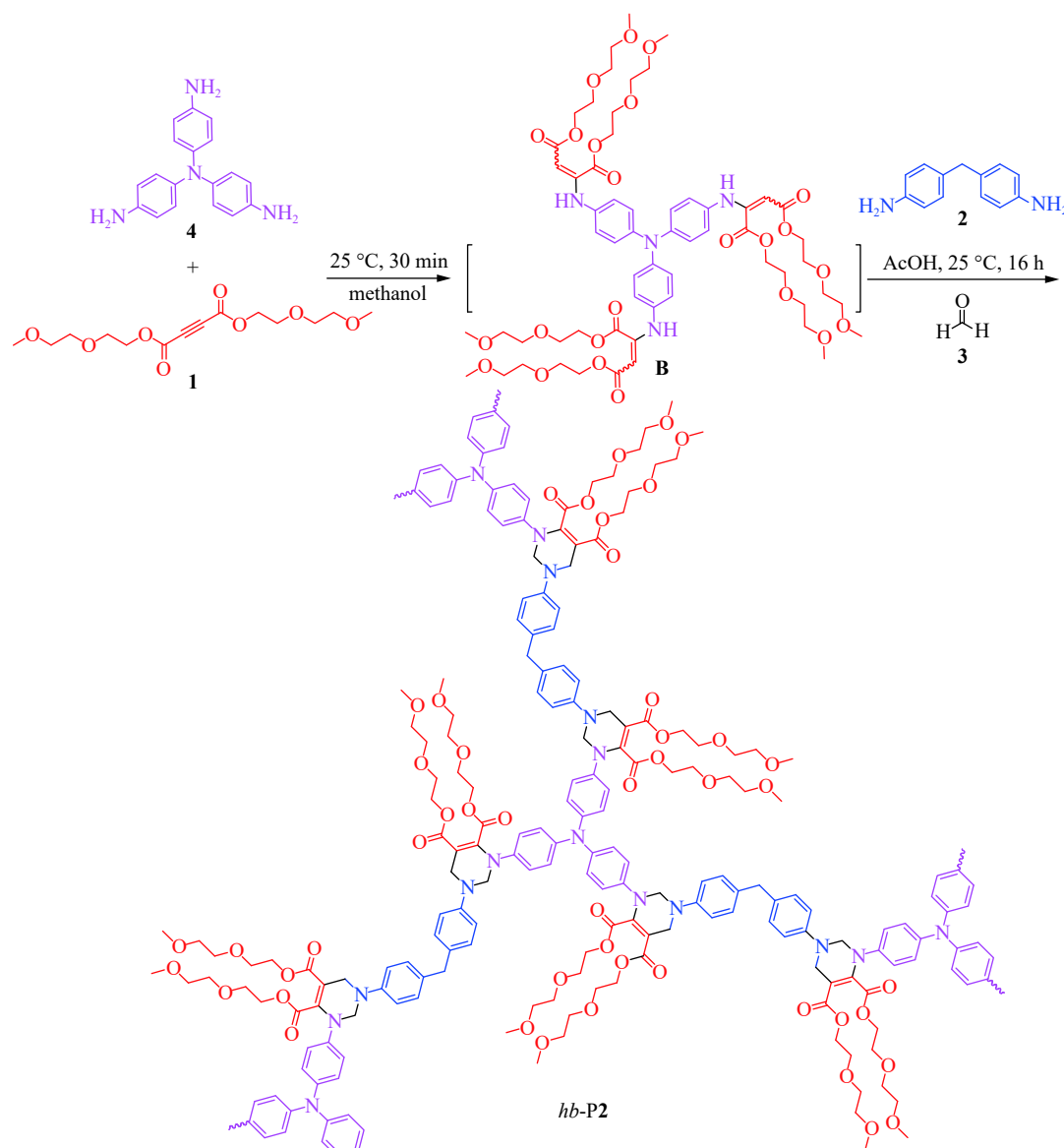### Design and Synthesis of Hyperbranched Polymers

One of the unique advantages of multicomponent polymerization is that through different monomer combinations, hyperbranched polymers with different topological structures can be obtained. Furthermore, through multicomponent tandem polymerization, the sequence of the functional units could be finely tuned in the polymer backbone. Attracted by these features of MCTP, the polymerization of activated alkyne, aromatic amine, and formaldehyde was utilized to synthesize hyperbranched polymers with different topologi-

cal structures and sequence of functional units. Firstly, ester group-activated internal alkyne **1** was synthesized as the key monomer, and its hydrophilic diethylene glycol monomethyl ether chain was designed to significantly improve the solubility of the product in methanol, ensuring the large molecular weight of the soluble product. A₂-type monomer 4,4′-methylenedianiline (**2**), A₃-type monomer tris(4-aminophenyl) amine (**4**), and A₄-type monomer tetrakis(4-aminophenyl)-methane (**5**) were then designed to polymerize with **1** and formaldehyde (**3**) through the above-mentioned MCTP with various combinations and loading sequence to afford hyperbranched poly(tetrahydropyrimidine)s with different topological structures and well-defined sequence of building blocks (Schemes 2−4).

The four-component tandem polymerization of activated alkyne **1**, aromatic diamine **2**, formaldehyde **3**, and aromatic triamine **4** was first investigated. As shown in Scheme 2, the hydroamination of internal alkyne **1** and diamine **2** was first carried out in methanol at room temperature in air with a molar ratio of [**1**]:[**2**] = 2:1 for 30 min to form the intermediate **A**, which was then reacted with the freshly added triamine **4** and formaldehyde **3** in the presence of acetic acid at room temperature for another 16 h to furnish hyperbranched poly(tetrahydropyrimidine) *hb*-P1 in 98% yield and a molecular weight (M_w) of 1.72×10^4 g/mol with good solubility. Through this tandem strategy, the diamine **2** and triamine **4** played different roles in the reaction and each contributed one type of nitrogen atom to the newly formed tetrahydropyrimidine rings. Hence, the chemical structure of *hb*-P1 is pre-designed and well-defined.

Through the tandem strategy, new hyperbranched polymers with different sequences of functional units could be facilely obtained by simply changing the feeding order of the monomers while keeping other reaction conditions and procedures unchanged. For example, if the internal alkyne **1** and triamine **4** were first reacted to generate intermediate **B** un-

Scheme 3   The synthesis of hyperbranched polymer *hb*-P2 through a one-pot MCTP
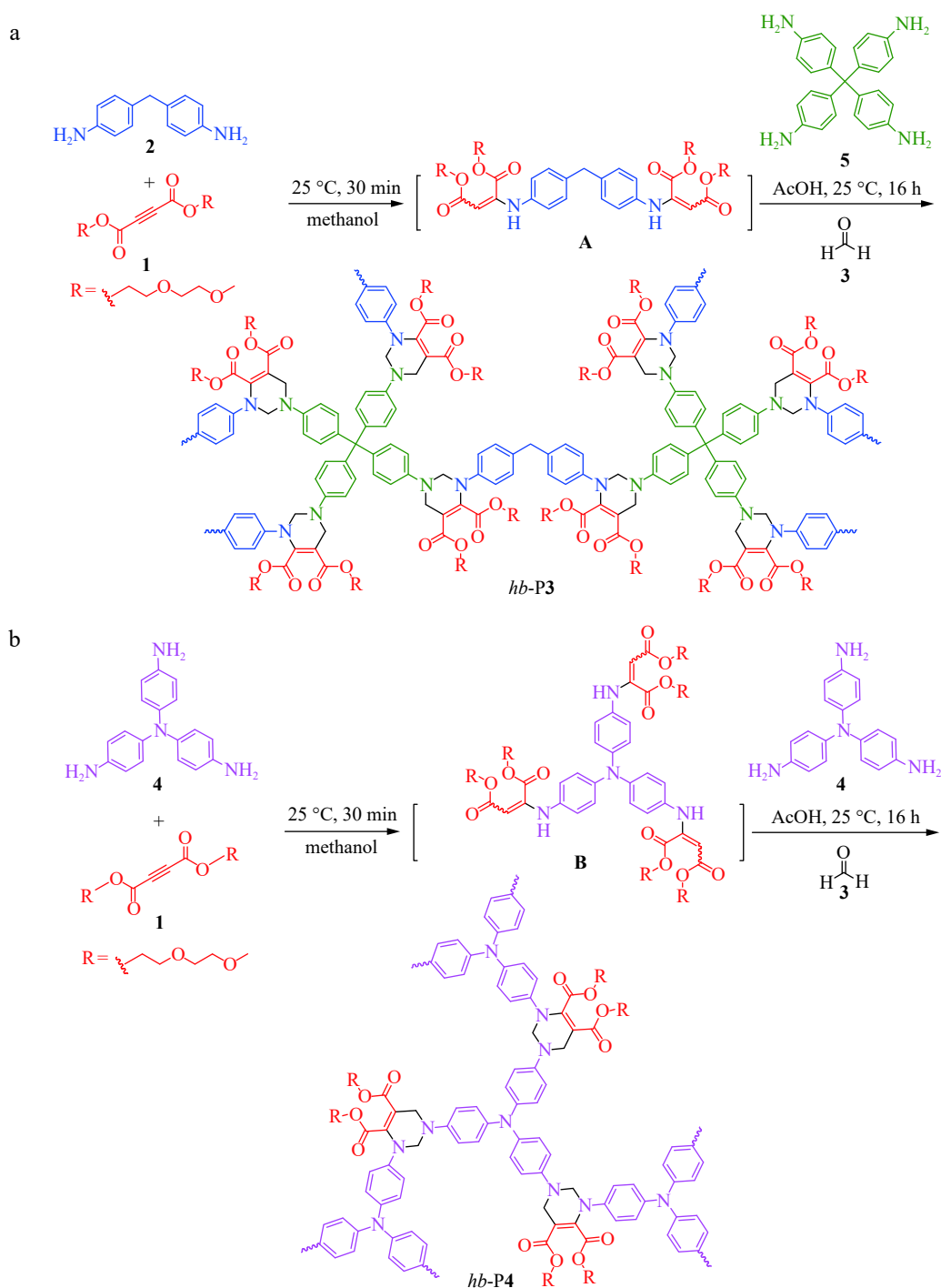
Scheme 4 The synthesis of hyperbranched polymers (a) *hb*-P**3** and (b) *hb*-P**4** through a one-pot MCTP

der similar condition at room temperature in methanol in air, the following reaction of newly added diamine **2** and formaldehyde **3** could produce hyperbranched poly(tetrahydropyrimidine) *hb*-P**2** in 84% yield and a M_w of 1.17 × 10^4 g/mol (Scheme 3). *hb*-P**2** shared similar chemical structure, component, and topological structure with *hb*-P**1**, but possessed different sequences of the diamine/triamine units.

Similarly, if tetraamine monomer **5** was adopted to replace triamine monomer **4** in the first MCTP shown in Scheme 2, *hb*-P**3** with totally different topological structu-

res could be obtained with 94% yield and a M_w of 2.24 × 10^4 g/mol (Scheme 4a). In addition, if triamine monomer **4** was used in both two steps, *hb*-P**4** with a unique topological structure could be gained with 95% yield and a M_w of 3.00 × 10^4 g/mol. Through simply tuning the monomer combination and loading sequence, a great diversity of hyperbranched polymers with different topological structures and functional unit sequences could be facilely accessed, demonstrating that this multicomponent tandem polymerization is a versatile synthetic platform.

Structure Characterization

Chemical structures of the hyperbranched poly(tetrahydro-pyrimidine)s *hb*-P**1**−**4** were characterized by spectroscopic techniques such as FTIR, ^{1}H-NMR, and ^{13}C-NMR spectroscopies through comparing with the spectra of monomers and model compound **7** (Scheme S1 in electronic supplementary information, ESI), which was prepared according to the literature.[41] For example, the FTIR spectra of **1**, **2**, **4**, **7**, and *hb*-P**1** are given in Fig. 1. The N−H stretching vibration bands of aromatic amine monomers **2** and **4** at ~3321 cm^{-1} were absent in the IR spectra of **7** and *hb*-P**1**, suggesting the NH$_2$ groups of **2** and **4** were completely consumed during the reaction or polymerization. One significant evidence to prove the product structure is that the C=O stretching vibration band of **1** at 1726 cm^{-1} had split into two different absorbance bands at ~1741 and 1691 cm^{-1} in both the spectra of **7** and *hb*-P**1**, which were originated from the two carbonyl groups on the newly formed tetrahydropyrimidine rings of the product with different chemical environments. A similar change was observed in the IR spectra of *hb*-P**2**−**4** as shown in Fig. S1 (in ESI), confirming their expected chemical structures.
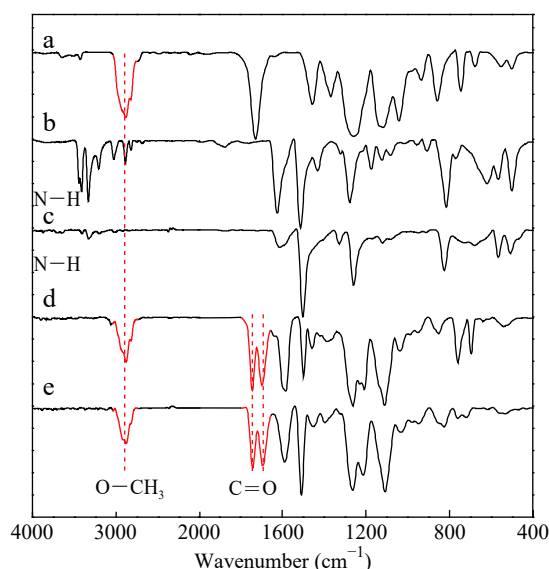

Fig. 1　IR spectra of (a) monomer **1**, (b) monomer **2**, (c) monomer **4**, (d) model compound **7**, and (e) *hb*-P**1**

The ^{1}H-NMR and ^{13}C-NMR spectra of **1**, **2**, **7**, and *hb*-P**1** are shown in Figs. 2 and 3 for example. Tris(4-aminophenyl)amine monomer **4** could not be well-dissolved in CDCl$_3$ and was not included. In the ^{1}H-NMR spectrum of *hb*-P**1**, the characteristic CH$_2$ resonance of **2** at δ = 3.77 ppm was observed at around 3.86 ppm, the CH$_3$ resonance of **1** at δ = 3.37 ppm was split into two signals at δ = 3.34 and 3.31 ppm, and two representative resonances emerged at δ = 4.26 and 4.80 ppm, which were assigned to the two kinds of newly formed CH$_2$ protons on the tetrahydropyrimidine rings. Similarly, in the ^{13}C-NMR spectrum of *hb*-P**1**, the CH$_2$ carbon signal of **2** at δ = 40.29 ppm was observed at δ = 40.74 ppm. The carbonyl signal of **1** at δ = 151.84 ppm was split into two signals at δ = 165.44 and 163.99 ppm, indica-

ting the change of chemical environment of the carbonyl groups after polymerization. Meanwhile, two new signals associated with the newly formed CH$_2$ carbons of the tetrahydropyrimidine ring emerged at δ = 103.36 and 48.12 ppm.
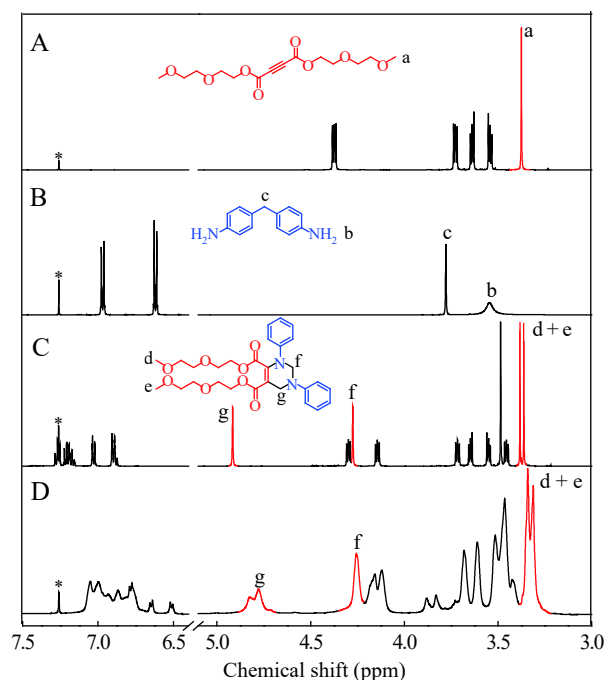

Fig. 2　^{1}H-NMR spectra of (A) monomer **1**, (B) monomer **2**, (C) model compound **7**, and (D) *hb*-P**1** in CDCl$_3$. The solvent peaks are marked with asterisks.

Fig. 3　^{13}C-NMR spectra of (A) monomer **1**, (B) monomer **2**, (C) model compound **7**, and (D) *hb*-P**1** in CDCl$_3$. The solvent peaks are marked with asterisks.
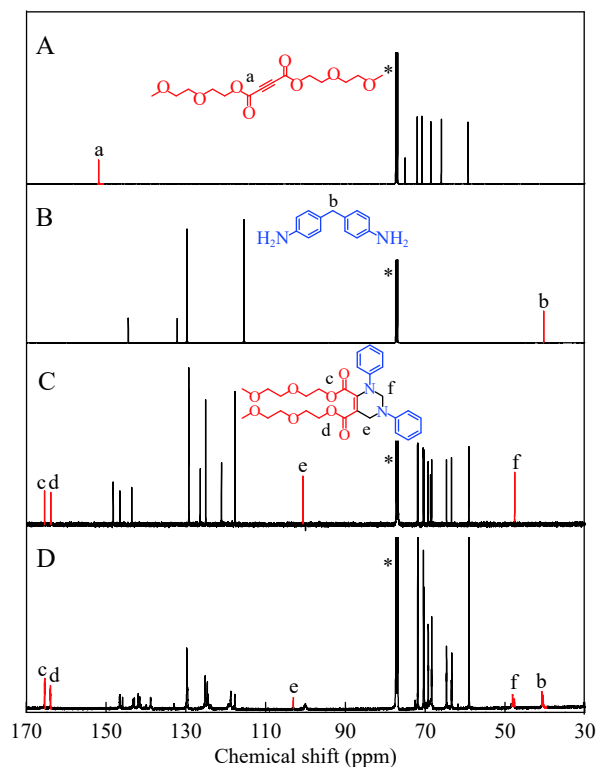
The characteristic signals all appeared in the ^{1}H-NMR spectra of *hb*-P**2**−**4** (Fig. S2 in ESI), and all these features matched well with the spectrum of the model compound **7** as well as the reported linear poly(tetrahydropyrimidine),[41] suggesting the expected hyperbranched polymer structures of *hb*-P**1**−**4**.

Aggregation-induced Emission Properties

Unique fluorescence behavior was reported for the model compound and the linear poly(tetrahydropyrimidine)s, even without any traditional luminophore with large conjugated structures. The photophysical properties of hyperbranched poly(tetrahydropyrimidine)s were hence investigated. The absorption maximum of model compound **7** in solution was reported at 316 nm, while its emission maximum in the condensed phase was reported at 513 nm.[41] The UV-Vis absorption spectra of THF solutions of *hb*-P**1**−**4** with a concentration of 54 mg/L suggested that their absorption maxima were located at 313 nm (*hb*-P**1**), 301 nm (*hb*-P**2**), 307 nm (*hb*-P**3**), and 317 nm (*hb*-P**4**), indicative of the absorption from the diphenyl-substituted tetrahydropyrimidine core structures (Fig. 4a). Both *hb*-P**2** and *hb*-P**4** exhibited an absorption shoulder at about 370 nm, because their electron-rich triphenyl amine moieties were directly conjugated with the electron-poor C=C double bonds on the tetrahydropyrimidine rings, bringing extended conjugation compared with the other two polymers.

The tris(4-aminophenyl)amine-containing hyperbranched polymers *hb*-P**1**, *hb*-P**2**, and *hb*-P**4** appeared as dark brown and non-emissive powder, probably due to the energy transfer between electron-rich triphenylamine moieties and the diphenyl-substituted tetrahydropyrimidine moieties. On the other hand, *hb*-P**3** could be well-dissolved in THF and methanol, while it possessed poor solubility in *n*-hexane. Under UV irradiation, the THF solution of *hb*-P**3** emitted faintly, while its solid thin film exhibited enhanced emission with the emission maximum located at 517 nm. The PL behavior of *hb*-P**3** was also studied in THF/hexane mixed solutions with different contents of *n*-hexane (Fig. S3 in ESI). When *n*-hexane was gradually added into the THF solution of *hb*-P**3**, the PL intensity was gradually enhanced and the emission maximum was red-shifted from 484 nm to 513 nm, owing to the formation of polymer nanoaggregates. The absolute fluorescence quantum efficiency (Φ_F) of *hb*-P**3** was measured by an integrating sphere, which suggested that the low Φ_F of the dilute *hb*-P**3** THF solution (Φ_F = 0.4%) could be obviously enhanced in THF/*n*-hexane mixture with 90 vol% *n*-hexane content (Φ_F = 2.0%) or in its thin film state (Φ_F = 3.0%). The typical aggregation-induced emission properties of *hb*-P**3** could also be evidenced by naked eye from the fluorescence images of the dilute THF solution, nanoaggregates in THF/*n*-hexane mixtures, and solid powder taken under UV irradiation. In this non-conjugated hyperbranched polymer, the large number of carbonyl groups and heteroatoms on the tetrahydropyrimidine rings were densely packed in the aggregated states, which might form "heteroatom clusters" to serve as the luminophore and emit fluorescence.[42]
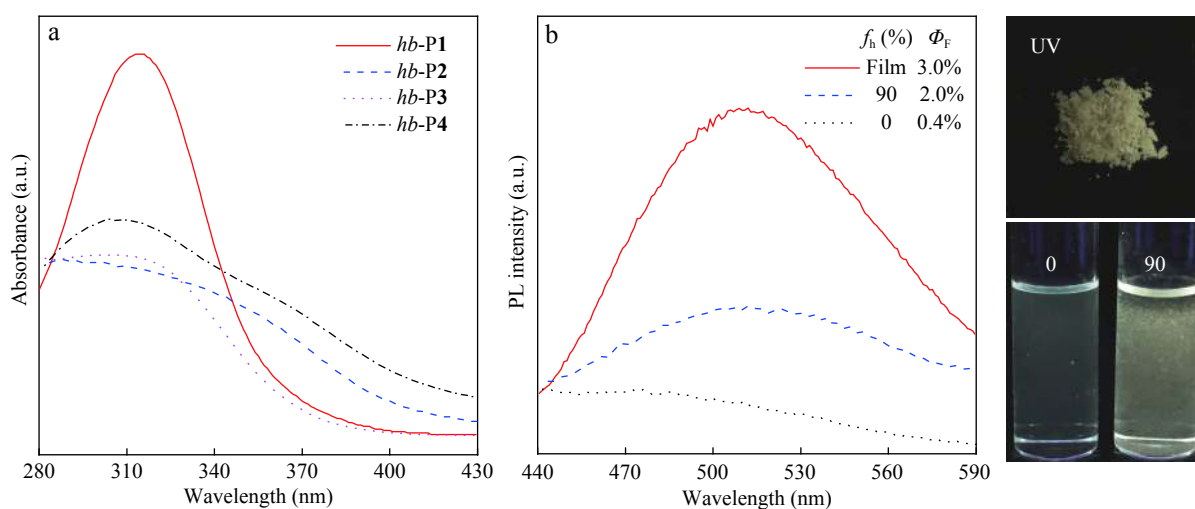

Fig. 4 (a) Absorption spectra of *hb*-P**1**−**4** in THF solutions (concentration: 54 mg/L); (b) PL spectra of *hb*-P**3** as a thin film and *hb*-P**3** in pure THF and THF/*n*-hexane solutions with 90 vol% *n*-hexane content and their fluorescence images under UV illumination (concentration: 5.4 mg/L). Absolute fluorescence quantum yield (Φ_F) was measured by an integrating sphere (excitation wavelength: 307 nm, emission wavelength: 517 nm)

CONCLUSIONS

In this work, four hyperbranched poly(tetrahydropyrimidine)s were designed and synthesized *via* a metal-free room temperature multicomponent tandem polymerization of ester group-activated internal alkyne, aromatic amine, and formaldehyde. Through different monomer combination strategies and the control of monomer loading sequence in two-step tandem processes, hyperbranched polymers with different topological structures as well as sequences of functional units were obtained in good to excellent yields and high molecular weights. The good solubility of the hyperbranched polymers enabled structural characterization by standard spectroscopic techniques. Aggregation-induced emission property was observed in one of the hyperbranched poly(tetrahydropyrimidine)s, which showed weak emission in solution but en-

hanced fluorescence in the aggregated states. The multi-component tandem polymerization may serve as a new synthetic method that provides a platform for developing AIE-active hyperbranched polymers with unique chemical and topological structures.

Ⓔ Electronic Supplementary Information

Electronic supplementary information (ESI) is available free of charge in the online version of this article at http://dx.doi.org/10.1007/s10118-019-2230-3.

ACKNOWLEDGMENTS

REFERENCES

1   Fréchet, J. M. J.; Hawker, C. J.; Gitsov, I.; Leon, J. W. Dendrimers and hyperbranched polymers: Two families of three-dimensional macromolecules with similar but clearly distinct properties. *J. Macromol. Sci. Part A* **1996**, *33*, 1399−1425.

2   Zhang, J.; Yong, H.; A, S.; Xu, Q.; Miao, Y.; Lyu, J.; Gao, Y.; Zeng, M.; Zhou, D.; Yu, Z.; Tai, H.; Wang, W. Structural design of robust and biocompatible photonic hydrogels from an *in situ* cross-linked hyperbranched polymer system. *Chem. Mater.* **2018**, *30*, 6091−6098.

3   Wu, W.; Tang, R.; Li, Q.; Li, Z. Functional hyperbranched polymers with advanced optical, electrical and magnetic properties. *Chem. Soc. Rev.* **2015**, *44*, 3997−4022.

4   Mu, B.; Liu, T.; Tian, W. Long-chain hyperbranched polymers: Synthesis, properties, and applications. *Macromol. Rapid Commun.* **2018**, 1800471.

5   Pedron, S.; Pritchard, A. M.; Vincil, G. A.; Andrade, B.; Zimmerman, S. C.; Harley, B. A. C. Patterning three-dimensional hydrogel microenvironments using hyperbranched polyglycerols for independent control of mesh size and stiffness. *Biomacromolecules* **2017**, *18*, 1393−1400.

6   Li, X.; Liu, X.; Shi, D.; Wei, W.; Chen, M.; Liu, X. Facile synthesis of hyperbranched polymers by sequential polycondensation. *ACS Macro Lett.* **2018**, *7*, 778−782.

7   Fletcher, N. L.; Houston, Z. H.; Simpson, J. D.; Veedu, R. N.; Thurecht, K. J. Designed multifunctional polymeric nanomedicines: Long-term biodistribution and tumour accumulation of aptamer-targeted nanomaterials. *Chem. Commun.* **2018**, *54*, 11538−11541.

8   Xu, Q.; A, S.; McMichael, P.; Creagh-Flynn, J.; Zhou, D.; Gao, Y.; Li, X.; Wang, X.; Wang, W. Double-cross-linked hydrogel strengthened by UV irradiation from a hyperbranched PEG-based trifunctional polymer. *ACS Macro Lett.* **2018**, *7*, 509−513.

9   Wang, D.; Zhao, T.; Zhu, X.; Yan, D.; Wang, W. Bioapplications of hyperbranched polymers. *Chem. Soc. Rev.* **2015**, *44*, 4023−4071.

10 Granskog, V.; Andrén, O. C. J.; Cai, Y.; González-Granillo, M.; Felländer-Tsai, L.; von Holst, H.; Haldosen, L. A.; Malkoch, M. Linear dendritic block copolymers as promising biomaterials for the manufacturing of soft tissue adhesive patches using visible light initiated thiol-ene coupling chemistry. *Adv. Funct. Mater.* **2015**, *25*, 6596−6605.

11 Fang, R.; Liu, Y.; Wang, Z.; Zhang, X. Water-soluble supramolecular hyperbranched polymers based on host-enhanced π-π interaction. *Polym. Chem.* **2013**, *4*, 900−903.

12 Fang, W.; Zhang, R.; Yao, Y.; Liu, H.; Chen, Y. Specific thermoresponsive behaviours exhibited by optically active and inactive phenylalanine modified hyperbranched polyethylenimines in water. *Chinese J. Polym. Sci.* **2017**, *35*, 1035−1042.

13 Yates, C. R.; Hayes, W. Synthesis and applications of hyperbranched polymers. *Eur. Polym. J.* **2004**, *40*, 1257−1281.

14 Sato, M.; Matsuoka, Y.; Yamaguchi, I. Preparation and properties of novel thermotropic liquid crystalline hyperbranched polyesters composed of five-membered heterocyclic mesogen by A$_2$ + B$_3$ approach. *J. Polym. Sci., Part A: Polym. Chem.* **2007**, *45*, 2998−3008.

15 Herzberger, J.; Niederer, K.; Pohlit, H.; Seiwert, J.; Worm, M.; Wurm, F. R.; Frey, H. Polymerization of ethylene oxide, propylene oxide, and other alkylene oxides: Synthesis, novel polymer architectures, and bioconjugation. *Chem. Rev.* **2016**, *116*, 2170−2243.

16 Tochwin, A.; El-Betany, A.; Tai, H.; Chan, K.; Blackburn, C.; Wang, W. Thermoresponsive and reducible hyperbranched polymers synthesized by RAFT polymerization. *Polymers* **2017**, *9*, 443.

17 McMahon, S.; Kennedy, R.; Duffy, P.; Vasquez, J. M.; Wall, J. G.; Tai, H.; Wang, W. Poly(ethylene glycol)-based hyperbranched polymer from RAFT and its application as a silver-sulfadiazine-loaded antibacterial hydrogel in wound care. *ACS Appl. Mater. Interfaces* **2016**, *8*, 26648−26656.

18 Zhao, B.; Zheng, Y.; Weng, Z.; Cai, S.; Gao, C. The electrophilic effect of thiol groups on thiol-yne thermal click polymerization for hyperbranched polythioether. *Polym. Chem.* **2015**, *6*, 3747−3753.

19 Han, J.; Zhao, B.; Tang, A.; Gao, Y.; Gao, C. Fast and scalable production of hyperbranched polythioether-ynes by a combination of thiol-halogen click-like coupling and thiol-yne click polymerization. *Polym. Chem.* **2012**, *3*, 1918−1925.

20 Chen, X.; Peng, L.; Feng, M.; Xiang, Y.; Tong, A.; He, L.; Liu, B.; Tang, Y. An aggregation induced emission enhancement-based ratiometric fluorescent sensor for detecting trace uranyl ion (UO$_2^{2+}$) and the application in living cells imaging. *J. Lumin.* **2017**, *186*, 301−306.

21 Yoshihara, D.; Noguchi, T.; Roy, B.; Sakamoto, J.; Yamamoto, T.; Shinkai, S. Design of a hypersensitive pH-sensory system created by a combination of charge neutralization and aggregation-induced emission (AIE). *Chem. Eur. J.* **2017**, *23*, 17663−17666.

22 Wu, J. L.; Zhang, C.; Qin, W.; Quan, D. P.; Ge, M. L.; Liang, G. D. Thermoresponsive fluorescent semicrystalline polymers decorated with aggregation induced emission luminogens. *Chinese J. Polym. Sci.* **2019**, DOI: 10.1007/s10118-019-2201-8.

23 Yu, L. Molecular design to regulate the photophysical properties of multifunctional TADF emitters towards high-performance TADF-based OLEDs with EQEs up to 224% and small efficiency roll-offs. *Chem. Sci.* **2018**, *9*, 1385−1391.

24 Shi, H.; Yang, J.; Dong, X.; Wu, X.; Zhou, P.; Cheng, F.; Choi, M. M. F. A Novel tetraphenylethene-carbazole type compound containing the dimesitylboron moiety: Aggregation-induced emission enhancement and electroluminescence properties. *RSC Adv.* **2014**, *4*, 19418−19421.

25 Li, Y.; Ma, Z.; Li, A.; Xu, W.; Wang, Y.; Jiang, H.; Wang, K.; Zhao, Y.; Jia, X. A single crystal with multiple functions of optical waveguide, aggregation-induced emission, and mechanochromism. *ACS Appl. Mater. Interfaces* **2017**, *9*, 8910−8918.

26 Zong, L.; Zhang, H.; Li, Y.; Gong, Y.; Li, D.; Wang, J.; Wang,

Z.; Xie, Y.; Han, M.; Peng, Q.; Li, X.; Dong, J.; Qian, J.; Li, Q.; Li, Z. Tunable aggregation-induced emission nanoparticles by varying isolation groups in perylene diimide derivatives and application in three-photon fluorescence bioimaging. *ACS Nano* **2018**, *12*, 9532−9540.

27 Qi, J.; Sun, C.; Li, D.; Zhang, H.; Yu, W.; Zebibula, A.; Lam, J. W. Y.; Xi, W.; Zhu, L.; Cai, F.; Wei, P.; Zhu, C.; Kwok, R. T. K.; Streich, L. L.; Prevedel, R.; Qian, J.; Tang, B. Z. Aggregation-induced emission luminogen with near-infrared-II excitation and near-infrared-I emission for ultradeep intravital two-photon microscopy. *ACS Nano* **2018**, *12*, 7936−7945.

28 Zou, J.; Lu, H.; Zhao, X.; Li, W.; Guan, Y.; Zheng, Y.; Zhang, L.; Gao, H. A multi-functional fluorescent probe with aggregation-induced emission characteristics: Mitochondrial imaging, photodynamic therapy and visualizing therapeutic process in zebrafish model. *Dyes Pigments* **2018**, *151*, 45−53.

29 Hong, Y.; Lam, J. W. Y.; Tang, B. Z. Aggregation-induced emission. *Chem. Soc. Rev.* **2011**, *40*, 5361−5388.

30 Hu, R.; Lam, J. W. Y.; Li, M.; Deng, H.; Li, J.; Tang, B. Z. Homopolycyclotrimerization of A₄-type tetrayne: A new approach for the creation of a soluble hyperbranched poly(tetraphenylethene) with multifunctionalities. *J. Polym. Sci., Part A: Polym. Chem.* **2013**, *51*, 4752−4764.

31 Hu, R.; Lam, J. W. Y.; Liu, J.; Sung, H. H. Y.; Williams, I. D.; Yue, Z.; Wong, K. S.; Yuen, M. M. F.; Tang, B. Z. Hyperbranched conjugated poly(tetraphenylethene): Synthesis, aggregation-induced emission, fluorescent photopatterning, optical limiting and explosive detection. *Polym. Chem.* **2012**, *3*, 1481−1489.

32 Zhang, J.; Shi, W.; Liu, Q.; Chen, T.; Zhou, X.; Yang, C.; Zhang, K.; Xie, Z. Atom-economical, room-temperature, and high-efficiency synthesis of polyamides *via* a three-component polymerization involving benzoxazines, odorless isocyanides, and water. *Polym. Chem.* **2018**, *9*, 5566−5571.

33 Zhang, J.; Wu, Y. H.; Wang, J. C.; Du, F. S.; Li, Z. C. Functional Poly(ester-amide)s with tertiary ester linkages *via* the Passerini multicomponent polymerization of a dicarboxylic acid and a diisocyanide with different electron-deficient ketones. *Macromolecules* **2018**, *51*, 5842−5851.

34 Tian, T.; Hu, R.; Tang, B. Z. Room temperature one-step conversion from elemental sulfur to functional polythioureas through catalyst-free multicomponent polymerizations. *J. Am. Chem. Soc.* **2018**, *140*, 6156−6163.

35 Xue, H.; Zhao, Y.; Wu, H.; Wang, Z.; Yang, B.; Wei, Y.; Wang, Z.; Tao, L. Multicomponent combinatorial polymerization *via* the Biginelli reaction. *J. Am. Chem. Soc.* **2016**, *138*, 8690−8693.

36 Tang, X.; Zheng, C.; Chen, Y.; Zhao, Z.; Qin, A.; Hu, R.; Tang, B. Z. Multicomponent tandem polymerizations of aromatic diynes, terephthaloyl chloride, and hydrazines toward functional conjugated polypyrazoles. *Macromolecules* **2016**, *49*, 9291−9300.

37 Jiang, R.; Liu, M.; Huang, H.; Huang, L.; Huang, Q.; Wen, Y.; Cao, Q.; Tian, J.; Zhang, X.; Wei, Y. Microwave-assisted multicomponent tandem polymerization for rapid preparation of biodegradable fluorescent organic nanoparticles with aggregation-induced emission feature and their biological imaging applications. *Dyes Pigments* **2018**, *149*, 581−587.

38 Long, Z.; Mao, L.; Liu, M.; Wan, Q.; Wan, Y.; Zhang, X.; Wei, Y. Marrying multicomponent reactions and aggregation-induced emission (AIE): New directions for fluorescent nanoprobes. *Polym. Chem.* **2017**, *8*, 5644−5654.

39 Deng, H.; Hu, R.; Zhao, E.; Chan, C. Y. K.; Lam, J. W. Y.; Tang, B. Z. One-pot three-component tandem polymerization toward functional poly(arylene thiophenylene) with aggregation-enhanced emission characteristics. *Macromolecules* **2014**, *47*, 4920−4929.

40 Zheng, C.; Deng, H.; Zhao, Z.; Qin, A.; Hu, R.; Tang, B. Z. Multicomponent tandem reactions and polymerizations of alkynes, carbonyl chlorides, and thiols. *Macromolecules* **2015**, *48*, 1941−1951.

41 Wei, B.; Li, W.; Zhao, Z.; Qin, A.; Hu, R.; Tang, B. Z. Metal-free multicomponent tandem polymerizations of alkynes, amines, and formaldehyde toward structure- and sequence-controlled luminescent polyheterocycles. *J. Am. Chem. Soc.* **2017**, *139*, 5075−5084.

42 Zhao, E.; Lam, J. W. Y.; Meng, L.; Hong, Y.; Deng, H.; Bai, G.; Huang, X.; Hao, J.; Tang, B. Z. Poly[(maleic anhydride)-*alt*-(vinyl acetate)]: A pure oxygenic nonconjugated macromolecule with strong light emission and solvatochromic effect. *Macromolecules* **2015**, *48*, 64−71.